Journal of Molecular Structure 979 (2010) 108–114

Contents lists available at ScienceDirect

Journal of Molecular Structure

journal homepage: www.elsevier.com/locate/molstruc

Synthesis, X-ray and spectroscopic analysis of 2-chloro-4-(methoxymethyl)-6-methyl-5-nitropyridine-3-carbonitrile

Marijana Jukić [a,*], Mario Cetina [b,**], Jasna Halambek [a], Ivana Ugarković [a]

[a] Department of Chemistry and Biochemistry, Faculty of Food Technology and Biotechnology, University of Zagreb, Pierottijeva 6, HR-10000 Zagreb, Croatia
[b] Department of Applied Chemistry, Faculty of Textile Technology, University of Zagreb, Prilaz baruna Filipovića 28a, HR-10000 Zagreb, Croatia

ARTICLE INFO

Article history:
Received 9 April 2010
Received in revised form 4 June 2010
Accepted 4 June 2010
Available online 12 June 2010

Keywords:
Substituted pyridine
X-ray diffraction
IR
NMR
UV–vis spectroscopy

ABSTRACT

Compound 2-chloro-4-(methoxymethyl)-6-methyl-5-nitropyridine-3-carbonitrile (**2**) has been obtained from 4-(methoxymethyl)-6-methyl-5-nitro-2-oxo-1,2-dihydropyridine-3-carbonitrile (**1**) by novel protocol using Vilsmeier–Haack chlorination and its solid state structure was analyzed using X-ray analysis. Structural features have been also studied by IR, NMR and electronic spectroscopy, and the optical properties were investigated by UV–vis absorption and fluorescence spectroscopy. Compound **2** crystallizes with two independent molecules in the asymmetric unit with almost identical geometric parameters. One C—H···O hydrogen bond self-assembles one type of independent molecule into chains, while second type is linked by one weak aromatic $\pi\cdots\pi$ stacking interaction. The absorption and fluorescence maximum of compound **2** were observed at 290 nm and 480 nm, respectively. The effects of solvents were investigated and interpreted on the emission spectra in protic and aprotic solvents in the range 200–600 nm.

1. Introduction

Heterocyclic compounds and their derivatives constitute a number of natural substances and are widely used in the synthesis of various biologically active compounds [1–3]. Among them, because of their chemical properties and biological activity, pyridine and their derivatives have attracted interest of many researches [4–7].

Different approaches in the construction of the pyridine skeleton with different substituents at various ring positions were examined, as well as relationship between the structure of these compounds and their biological activities [8–12]. In particular, certain derivatives of pyrimidines, being an integral part of DNA and RNA, exhibit diverse pharmacological activities such as antimicrobial, antifungal, antibacterial, pesticidal [13–17]. Pyridine derivatives are widely used as antiallergic [18], antihypertensive [19], bronchodilators [18], antitumor [8,18], and analgesic and muscle relaxant (interneuronal blocking) agents [20]. The pyridine ring forms the basis of a large number of pharmacological products such as vitamin B5, vitamin B6, pyridoxal and pyridoxamine; and drugs such as nifedipine (cardiovascular), nichetamide (analgesics), sulphapyridine (sulfonamide), lacidipine (antihypertensive), proflavine (antiseptics) and therefore is considered a privileged structure in the pharmaceutical industry [7,21–24].

Substituted pyridine compounds such as 2-halo-substituted pyridines are useful as intermediates for preparing insecticides, herbicides and pharmaceuticals. Preliminary examination demonstrates in vitro antitubercular and antifungal activity of chloropyridine which are finding as a new class of antimicrobial agents [25]. Halogen-substituted 2-pyridones are also key intermediates for metalcatalyzed coupling reactions, because the chlorine atom at position 2 is fairly reactive and may easily be replaced by various groups under nucleophilic attack [26].

The prominent role played by pyridines and related compounds as privileged structures in many natural products and bioactive compounds, led us to consider the extension of our studies to the pyridine nucleus. The present work has been undertaken as a part of our systematic research on the synthesis and analysis of heterocyclic molecules [27–30], and continues our investigation of structures these bioactive compounds and their metal complexes. The goal of this work was to carry out further characterization of various derivatives of pyridines. Particularly, we wanted to determine how the position and number of substituent modulate their spectroscopic properties. To evaluate the relationship between biological activity and molecular structure, the knowledge of their electronic structure and spectral properties are particularly important. Therefore, in the present work, we have reported the synthesis, structure and spectroscopic properties of 2-chloro-4-(methoxymethyl)-6-methyl-5-nitropyridine-3-carbonitrile.

* Corresponding author. Tel.: +385 1 4605 282; fax: +385 1 4836 083.
** Corresponding author. Tel.: +385 1 3712 590; fax: +385 1 3712 599.
E-mail addresses: mjukic@pbf.hr (M. Jukić), mario.cetina@ttf.hr (M. Cetina).

0022-2860/$ - see front matter © 2010 Elsevier B.V. All rights reserved.
doi:10.1016/j.molstruc.2010.06.012

2. Experimental

2.1. General methods

All reactions were performed with commercially available reagents and they were used without further purification, and the solvents were distilled and dried by standard procedures.

The reaction course and purity of the products were checked by thin-layer chromatography (TLC) on Merck, DC-Alufolien Kieselgel 60 F254, using dichloromethane–ethyl acetate as the eluent. Investigated compound was purified by preparative thin-layer chromatography on silica gel (Merck, Kieselgel 60 HF254) using the mixtures CH_2Cl_2:EtOAc (3:1 v/v) and by recrystallization from (aqueous) EtOH. The solvents were of spectroscopic grade.

The chemical structure and the purity of the compound were confirmed by melting points, FTIR, ^{1}H and ^{13}C NMR spectra. The melting points were determined using an electrothermal Buechi apparatus and are not corrected. The IR spectra were recorded for KBr pellets with a Bomem MB 100 mid FTIR spectrophotometer. The ^{1}H and ^{13}C NMR spectra were recorded on on a Bruker Avance 300 or Bruker Avance 600 MHz spectrometer in DMSO-d_6 solution with Me_4Si as internal standard. Ultraviolet absorption spectra of synthesized compound have been recorded in the region 200–600 nm using an Ocean optics USB 4000 spectrophotometer and fluorescence spectra were recorded with Varian Cary fluorescence spectrophotometer at wavelength of maximum absorption (λ_{max}). The effects of solvents were investigated on the emission spectra in six different solvents in methanol, ethanol, tetrahydrofuran, N,N-dimethylformamide, 1,2-dichloroethane and heptane. The UV–vis spectra were obtained at room temperature and fluorescence spectra at 25 ± 0.1 °C, both using 1 cm optical path-length quartz cells.

2.2. Synthesis

2.2.1. Preparation of 2-chloro-4-(methoxymethyl)-6-methyl-5-nitropyridine-3-carbonitrile (**2**)

2.23 g (10 mmol) of 4-(methoxymethyl)-6-methyl-5-nitro-2-oxo-1,2-dihydropyridine-3-carbonitrile (**1**) in 15 mL dry DMF were cooled to 0–5 °C, phosphorus oxychloride (2.8 mL, 30 mmol) was added dropwise and then allowed to stand until no further heat of reaction was noticeable. A thick brown suspension remained at the end of the exothermal reaction. The reaction mixture was than heated to 55 °C for 2 h with stirring, while the reaction monitoring was carried out by TLC. After completion, the reaction mixture was added to cold, poured on crushed ice (40 g), slowly with constant stirring, and then brought to pH ≈ 7 using saturated solution of sodium hydrogen carbonate and extracted with dichloromethane. The organic layer was washed with water, dried over anhydrous Na_2SO_4, and evaporated under reduced pressure to afford the crude product. The crude residue was purified on silica gel column chromatography over silica gel using dichloromethane/ethyl acetate (4:3) as eluent to give the title compound as a crystalline solid (yield 89%, m.p. 75–78 °C). Elemental analysis, calculated for $C_9H_8N_3O_3Cl$ (241.6323); % C 44.74; % H 3.34; % N 17.39. Found: % C 44.69; % H 3.39; % N 17.31; IR (KBr) ν: 3083–3052 cm^{-1} (aromatic C—H), 3004, 2822 (aliphatic C—H), 2236 (C≡N), 1614 (C=C), 1585 (C=N), 1545, 1359 (C—NO_2), 1266 (C—N), 1110 (Ar—Cl), 781 (C—Cl) cm^{-1}; ^{1}H NMR (DMSO-d_6) δ: 4.69 (2H, s, CH_2O), 3.29 (3H, s, OCH_3), 2.50 (3H, s, CH_3, C-6) ppm; ^{13}C NMR, APT (DMSO- d_6) δ: 153.65 (*C*-5), 152.48 (*C*-4), 147.09 (*C*-2); 144.20 (*C*-3); 113.12 (*C*-6), 109.33 (C≡N); 68.83 (OCH_2); 59.54 (OCH_3); 21.22 (CH_3) ppm.

Table 1
X-ray crystallographic data for **2**.

Formula	$C_9H_8ClN_3O_3$
Formula weight	241.63
Crystal size (mm)	0.36 × 0.38 × 0.65
Crystal colour, shape	Colourless, block
Crystal system	Monoclinic
Space group	$P2_1/c$
Unit cell dimensions	
a ()	8.1865(4)
b ()	30.8169(8)
c ()	9.9032(4)
β (°)	118.291(5)
V (^{3})	2199.97(15)
Z	8
$D_{calc.}$ (g cm^{-3})	1.459
Absorption coefficient, μ (mm^{-1})	0.343
Scan mode	ω
θ range (°)	3.97–28.00
Index ranges	$-10 \leqslant h \leqslant 10$ $-40 \leqslant k \leqslant 40$ $-13 \leqslant l \leqslant 12$
Collected reflections No.	27,829
Independent reflections No./$R_{int.}$	5297/0.0348
Reflections No. $I \geqslant 2\sigma(I)$	3098
Data/restraints/parameters	5297/0/293
Goodness-of-fit on F^2, S	1.037
R [$I \geqslant 2\sigma(I)$]/R [all data]	0.0506/0.0922
wR [$I \geqslant 2\sigma(I)$]/wR [all data]	0.1378/0.1642
Max./min. electron density (e^{-3})	0.338/−0.280

2.3. Crystal structure determination

Single crystal of **2** suitable for X-ray single crystal analysis was obtained at room temperature by partial evaporation from ethanol solution. The intensities were collected at 295 K on a Oxford Diffraction Xcalibur2 diffractometer with Sapphire3 detector using graphite-monochromated Mo K radiation (λ = 0.71073 Å). *CrysAlis* [31] programs were used for data collection and reduction. The crystal structure was solved by direct methods [32]. All non-hydrogen atoms were refined anisotropically by full-matrix least-squares calculations based on F^2 [32]. All hydrogen atoms were included in calculated positions as riding atoms, with *SHELXL97* [32] defaults. Details of crystal data, data collection and refinement parameters are given in Table 1. *PLATON* [33] program was used for structure analysis and drawings preparation. CCDC 771895 contains the Supplementary crystallographic data for this paper. These data can be obtained free of charge from The Cambridge Crystallographic Data Centre via www.ccdc.cam.ac.uk/data_request/cif.

3. Results and discussion

3.1. Synthesis

2-chloro-4-(methoxymethyl)-6-methyl-5-nitropyridine-3-carbonitrile (**2**), was synthesised by treatment of starting compound, 4-(methoxymethyl)-6-methyl-5-nitro-2-oxo-1,2-dihydropyridine-3-carbonitrile (**1**), with a strong chlorinating agent, such as the Vilsmeier–Haack mixture of phosphorous oxychloride and N,N-dimethylformamide, using three equivalents of $POCl_3$ in excess (Scheme 1). The reaction was conducted under anhydrous conditions, because if the water was present there would be the need to use additional amounts of phosphorus oxychloride which is depleted in the presence of water.

Under conventional heating conditions, this substitution reaction is typically carried out at elevated temperatures using $POCl_3$ in excess. This reagent has also proven successful for chlorination of hydroxy substituted 2-pyridones [34,35]. Glasnov et al. showed that this transformation could be effectively performed with

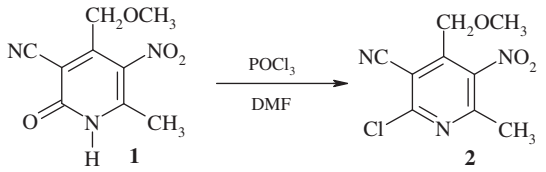

Scheme 1. Synthesis of the pyridine derivative **2.**

microwave irradiation using dioxane as solvent and only two equivalents of $POCl_3$ [36].

Transformation of the compound **1** by boiling in $POCl_3$ gave 2-chloro-4-(methoxymethyl)-6-methyl-5-nitropyridine-3-carbonitrile (**2**) which is a key compound for various transformations because this compound reacts smoothly with pyridine with the formation of a pyridylpyridinium salt, which is a promising starting material for the synthesis of various pyridine derivatives, including condensed pyridines [37]. The improvement in product yield shows the advantage of this reaction compared to the conventional Harris–Folkers [38] procedure.

3.2. X-ray crystal structure analysis

Compound **2** crystallized in monoclinic space group $P2_1/c$ with two independent molecules in the asymmetric unit (Fig. 1).

All equivalent bond lengths in two independent molecules are within 3σ values, with the exception of N3—C5 and C4—C5 bond lengths which differ for 4σ and 5σ values, respectively (Table 2). We compared this structure with 2-chloro-3-cyano-pyridines in which carbon atom substituent is bonded to C4 atom of the pyridine ring. An analysis revealed that there are only two major differences in bond lengths between **2** and five closely related structures [39–43]. Thus, C2—Cl1 bond in 2-chloro-3-cyano-6-phenyl-4-*p*-tolylpyridine [40] is *ca.* 0.035 Å longer [1.754(3) Å] than equivalent bond in **2**. The same bond in 2-chloro-3-cyano-6-methyl-5-nitropyridine derivative [42], which has identical substituents at the C2, C3, C5 and C6 atoms of the pyridine ring, is *ca.* 0.040 Å shorter [1.681(6) Å] compared to **2**. Furthermore, two N—O bond lengths of nitro group differ for almost 0.05 Å [1.189(8); 1.236(8) Å] in this

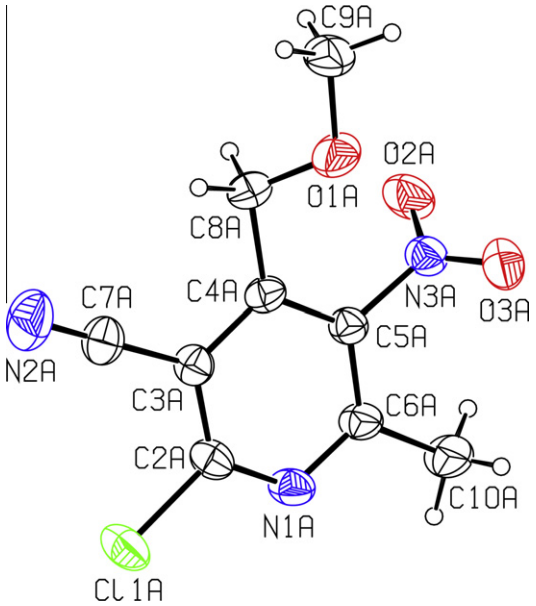

Fig. 1. A molecular structure of **2**, with the atom-numbering scheme. For clarity, only one of two independent molecules in the asymmetric unit is shown. Displacement ellipsoids for non-hydrogen atoms are drawn at the 30% probability level.

Table 2
Selected bond lengths (Å) and bond angles (°) for compound **2**.

N1—C2	1.313(3)	C4—C5	1.375(3)
	1.316(3)		1.390(3)
C2—Cl1	1.720(2)	C5—N3	1.476(3)
	1.720(2)		1.465(3)
C2—C3	1.393(3)	N3—O2	1.212(2)
	1.398(3)		1.211(3)
C3—C7	1.433(3)	N3—O3	1.213(2)
	1.439(3)		1.214(2)
N2—C7	1.135(3)	C5—C6	1.389(3)
	1.130(3)		1.387(3)
C3—C4	1.398(3)	C6—N1	1.332(3)
	1.391(3)		1.337(3)
C4–C8	1.513(3)	C6—C10	1.499(3)
	1.504(3)		1.503(3)
N1—C2—C3	124.6(2)	C4—C5—N3	120.17(19)
	124.38(19)		119.98(17)
N1—C2—Cl1	116.22(17)	C5—N3—O2	116.5(2)
	116.27(15)		117.05(18)
Cl1—C2—C3	119.16(17)	C5—N3—O3	118.1(2)
	119.33(15)		118.44(19)
C2—C3—C7	120.7(2)	O2—N3—O3	125.3(2)
	120.09(19)		124.5(2)
C2—C3—C4	118.22(19)	N3–C5–C6	117.14(18)
	118.67(17)		117.33(17)
C7—C3—C4	121.0(2)	C5—C6—C10	123.6(2)
	121.23(18)		123.17(19)
C3—C4—C5	115.89(19)	C5—C6—N1	120.40(19)
	115.59(17)		120.32(18)
C3—C4—C8	120.78(19)	C10—C6—N1	115.9(2)
	120.88(18)		116.48(19)
C8—C4—C5	123.3(2)	C6—N1—C2	118.26(19)
	123.52(18)		118.31(17)
C4—C5—C6	122.6(2)		
	122.63(18)		

very similar structure [42], and the group is almost perpendicular with respect to the pyridine ring with dihedral angle of 77.6(7)°. In **2**, two N—O bond lengths are within standard uncertainties, and two almost identical dihedral angles are approximately 8° smaller [69.9(3)°; 69.8(3)°] compared to the angle in former structure [42].

There is only one intermolecular hydrogen bond in **2**, linking only B independent molecules (Figs. 2 and 3). The C8B···O3B hydrogen bond self-assembles the molecules into $C(6)$ chains [44] parallel to the *c* axis [C8B···O3B = 3.157(3) Å; H···O3B = 2.51 Å; C8B—H···O3B = 124°. It is well known that strength of C—H···O hydrogen bond generally depends on the carbon hybridisation and acidity. In general, methylene group is not consider very acidic. However, carbon acidity increases and hydrogen bond is shorter if carbon atom is surrounded with electron-withdrawing atoms or groups [45]. This effect is often called 'activation' of C—H, although non-activated C—H groups may also act as donors [46].

One weak aromatic $\pi\cdots\pi$ stacking interaction [47] between pyridine rings of the neighboring A independent molecules participates also in supramolecular aggregation (Fig. 3). An interplanar angle between the rings is 0°, interplanar spacing is 3.8738(11) Å, a centroid separation 4.3306(16) Å, and corresponding centroid–centroid offset *ca* 1.94 Å. This $\pi\cdots\pi$ interaction links A independent molecules into dimers. Thus, the molecules of **2** are self-assembled by two different types of intermolecular interactions, C—H···O hydrogen bond and $\pi\cdots\pi$ interaction, so forming such supramolecular structure in which A and B molecules are not mutually connected by any other type of intermolecular interaction.

3.3. Spectral analysis

3.3.1. IR absorption spectra

The spectroscopic characterization of compound **1** is published [30]. In the infrared spectra (in KBr) of compound **2** the band cor-

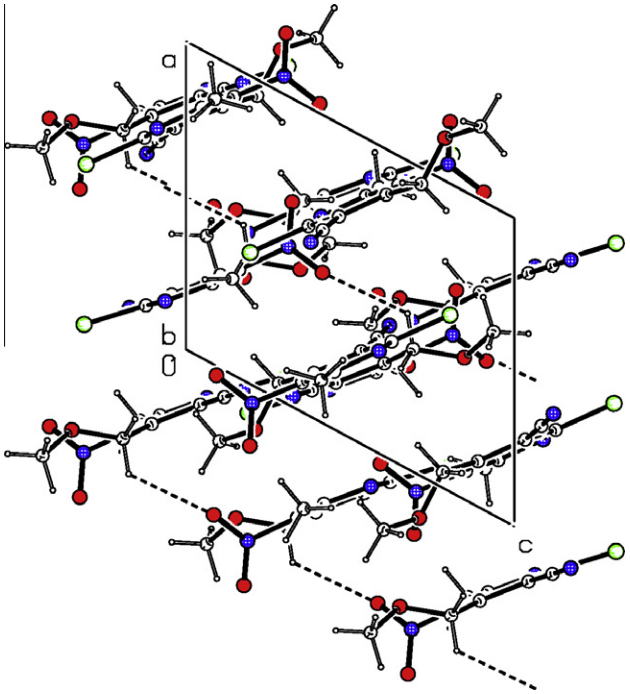

Fig. 2. A crystal packing diagram of **2**, viewed along the *b* axis, showing parallel arrangement of molecules and C—H···O hydrogen bond which links B independent molecules into infinite chains. Hydrogen bonds are indicated by dashed lines.

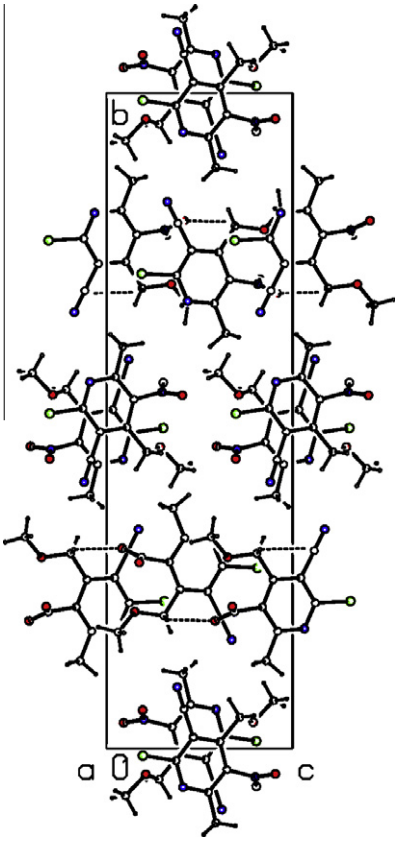

Fig. 3. A crystal packing diagram of **2**, viewed along the *a* axis, showing C—H···O hydrogen bond and pyridine rings' stacking of A molecules. Hydrogen bonds are indicated by dashed lines.

responding to the imino group ν(N—H) vibrations, which was recorded in the region 3312 cm^{-1} for the compound **1** [30], is absent.

The IR spectra of compound **2** showed medium bands at 3083–3052 cm^{-1} and 3004–2839 cm^{-1}, which are attributed to the vibrations of the aromatic (C—H) and aliphatic (C—H) bonds. Strong band observed in the region at 2236 cm^{-1} in the IR spectra is assignable to the carbonitrile ν(C≡N) stretching vibrations.

The presence of the band at 1658 cm^{-1} which is assigned to stretching vibrations ν(C=O) of the ring, as well as the band at 1578 cm^{-1} assigned to ν(N—H) bending vibration of ring which where observed for compound **1** in the spectra for compound **2** is also absent [30].

The band due to the skeleton deformation of stretching modes pyridine ν(C=C) and ν(C=N) bands in the region 1614–1585 cm^{-1} were recorded. In the region 1545–1359 cm^{-1} interesting features are observed for the (–NO_2) symmetric stretch. The –(–NO_2) symmetric stretching mode is split into a doublet due to the existence of non-equivalent molecules in the unit cell. The (–NO_2) band should be split into three components and these values are in accordance with the literature [48,49].

The IR spectrum of the derivative **2** contains a medium absorption band at 1110 cm^{-1} which belongs to (Ar—Cl), indication for the halogen on aromatic structure. The C—Cl stretching vibrations give rise to strong absorptions in the range 781 cm^{-1}.

3.3.2. NMR spectra

The ^{1}H NMR spectrum of investigated compounds measured in DMSO-d_6 at 25 °C show a signals from the starting pyridone **1,** and the absence of the broad singlet signal approximately at 13 ppm corresponding to N*H* protons. Two singlets at 4.69 ppm are attributed to two methylene protons of –CH_2–O–CH_3 group.

Similarly, multiple's appearing at 3.29 ppm account for protons due to methoxy groups –O–CH_3 (C-4) downfield resonating D_2O exchangeable signal integrating for three protons, respectively. The singlet at 2.50 ppm is corresponding for methyl groups (C-6) three protons.

The structures of the title compound are further substantiated by the ^{13}C APT NMR, spectroscopic data measured in DMSO-d_6. The spectroscopic data of compound **2** indicate that the carbons atoms give rise to different peaks within the frequency range of 21.22–153.65 ppm. Compared with the starting material **1** [30], as expected, significant changes are observed for chemical shift values of quaternary carbons signals assignable to *C*O of the *C*O—NH amide group which disappeared approximately from 160.93 ppm.

Quaternary carbons signals is observed in the ^{13}C APT NMR spectrum of compound **2** at 153.65 ppm (C-5), 152.48 ppm (C-4), 147.09 ppm (C-2), 144.20 ppm (C-3), 113.12 ppm (C-6) and at 109.33 ppm (*f*≡N), respectively.

Singlet is observed for secondary methylene carbons of –*C*H_2–O–CH_3 group of compound **2** at 68.83 ppm. Similarly, two singlets at 59.54 and 21.22 ppm, respectively are attributed to primary carbons of methyl group.

The results inferred from the IR and NMR spectral data of compound **2** are found to be in agreement with the proposed structure and supported also by X-ray diffraction data.

3.3.3. UV–vis and fluorescence spectra

The UV–vis electronic spectra of 2-chloro-4-(methoxymethyl)-6-methyl-5-nitropyridine-3-carbonitrile (**2**) have been recorded in protic and aprotic organic solvents within 200–600 nm range. The effects of the electron-withdrawing properties of halogen substituent and solvents on the absorption and fluorescence spectra was investigated and interpreted.

A dilute ethanolic solution of the compound **2** (c (**2**) = 4.0144×10^{-4} mol dm^{-3}) at 25 ± 0.1 °C was prepared and pipetted into a standard 1 cm square fluorescence cell. Prescan

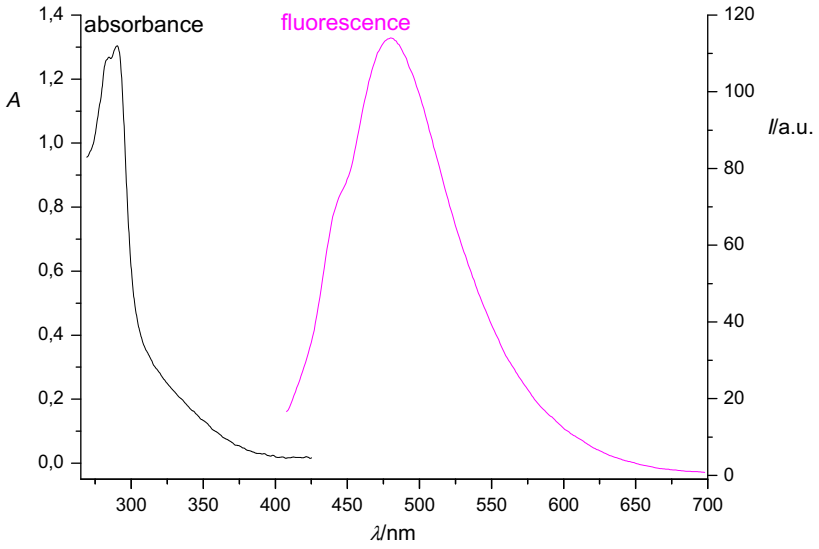

Fig. 4. Absorption and emission spectrum of **2** in 95% ethanolic solution (c (**2**) = 4.0 × 10^{-4} mol dm^{-3} at 25 ± 0.1 °C (prescan λ_{ex} = 390 nm)).

Table 3
Fluorescence data of **2** recorded in protic and aprotic solvents at the concentration of c (**2**) = 40 × 10^{-4} mol dm^{-3} at 25 ± 0.1 °C (λ_{ex} = 390 nm); λ_s is wavelength of 'shoulder'.

Solvent	λ_{max} (nm)	ε_{max} (10^6 dm^3 mol^{-1} cm^{-1})	λ_s (nm)
Tetrahydrofuran	467	1.11	–
1,2-dichloroethane	460	0.814	442
N,N-dimethylformamide	487	0.661	441
Ethanol	480	0.285	445
Heptane	442	0.161	464
Methanol	484	0.101	444

was used to determine the optimal excitations wavelength. The wavelength λ_{ex} = 390 nm was then selected for study.

As can be seen from Fig. 4, in the UV spectra of the 2-chloro-4-(methoxymethyl)-6-methyl-5-nitropyridine-3-carbonitrile (**2**) the absorption maxima is obtained at 290 nm (λ_{max} (**2**) = 290.1 nm), while the fluorescence emission spectrum peak is recorded at 480 nm (λ_{max} (**2**) = 480 nm) and is red-shifted with respect to the absorption spectrum. That absorption maxima correspond to a π–π^* transition of the conjugated system within the aromatic pyridine ring, and are in agreement with literature data. Pyridine shows an electronic transition at 257 nm because of the π–π^* excitation for non-conjugated derivatives, and shifted to longer wavelengths when substituents are conjugated to the aromatic system [50].

The λ_{max} of the UV absorption spectrum of compound **2** is hypsochromically shifted by about 40 nm to 290 nm from that of the starting 2(1H)-pyridone (**1**) spectrum (λ_{max} (**1**) = 331 nm [30].

Electron-withdrawing substituent (–Cl) have significant effect on the position of emission band of compound **2,** bathochromically shifting the maximum of the UV absorption bands for $\Delta\lambda_{max}$ = 82 nm, from that of the compound **1,** and producing a hypochromic effect which results in decreased emission intensity ($\Delta\varepsilon_{max}$ = −0.226 × 10^6 dm^3 mol^{-1} cm^{-1}). This is in agreement with literature data that an auxochrome containing unshared electrons which when attached to the chromophore changes both the intensity as wells the wavelength of the absorption and emission maximum [51]. The decrease in the molar absorptivity (ε) observed here can be related to the effect of the overlap of the orbitals involved in the electronic excitation. Excitation of one electron from the

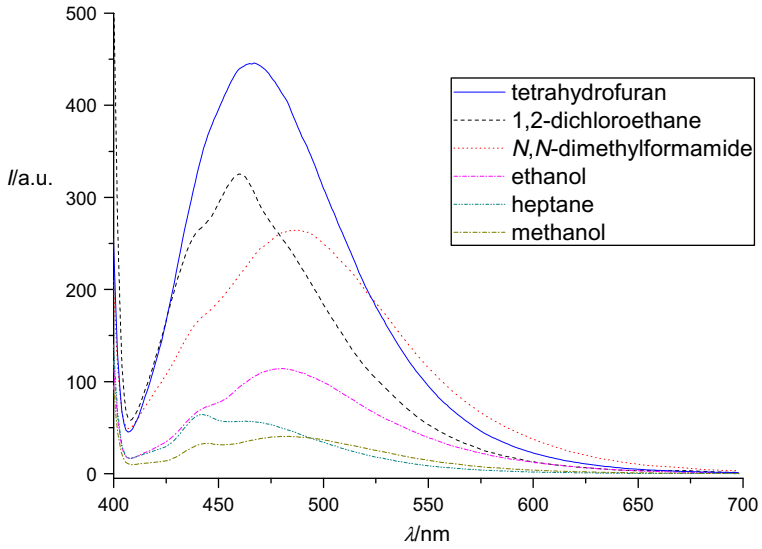

Fig. 5. Fluorescence spectra of **2** in protic and aprotic solvents at 25 ± 0.1 °C(c (**2**) = 4.0 × 10^{-4} mol dm^{-3}; λ_{ex} = 390 nm).

lone par present on the heteroatom to an antibonding π^* orbital ($n \rightarrow \pi^*$), so called "forbidden" transition is lower in energy than the $\pi \rightarrow \pi^*$ "allowed" transition, but the molar absorptivity of the "forbidden" transition is a thousand times smaller than "allowed" transition [51]. The effects of halogen substituent which contain unshared electrons with the electron-withdrawing properties attached to the aromatic ring change both the intensity as wells the wavelength of the absorption and emission maximum even can diminish or destroy fluorescence [52]. This effect can be from "forbidden" transitions which are related to the effect of the overlap of the orbital involved in the electronic excitation.

Because the substituent effects appear to exert a more pronounced effect on emission than on absorption spectra [53], we examined the fluorescence spectra of compound **2**, which have been measured in six solvents of different polarity and hydrogen bonding donor ability such as methanol, ethanol, tetrahydrofuran, N,N-dimethylformamide, 1,2-dichloroethane and heptane. The concentrations were the same and the measurements were taken at room temperature. The ultraviolet emission wavelength of the electronic transitions of the examined compounds are given in Table 3, and representative spectra are shown in Fig. 5.

It can be seen from Table 3 that 2-chloro-4-(methoxymethyl)-6-methyl-5-nitropyridine-3-carbonitrile (**2**) showed the highest fluorescence intensity in tetrahydrofuran. The emission spectra of compounds **2** in DMF is little bathochromically shifted ($\Delta\lambda_{max}$ = 7 nm) with respect to the emission spectra in EtOH. It was also observed that the emission spectra of compound **2** in all aprotic solvents except DMF is hypsochromically shifted with respect to the spectra in protic solvents such as ethanol or methanol which is in agreement with literature data that the transitions of polar bands are affected by solvent polarity. As solvent polarity is increased $\pi \rightarrow \pi^*$ bands undergo red shifts so since excited state is more polar than the ground state, and hence stabilization is greater relative to the ground state in polar solvents [51].

Visible emission maxima of the compound **2** (Table 3) showed bathocromic ($\Delta\lambda_{max}$ = 45 nm) and hypochromic ($\Delta\varepsilon_{max} = -1.009 \times 10^6$ dm^3 mol^{-1} cm^{-1}) shifts, as the solvent polarity increases which results in decreased emission intensity, and the fluorescence efficiencies are reduced.

Furthermore, a minor shoulder emission located at around 450 nm was observed for compound **2** in both, protic and aprotic solvents, except THF (Fig. 5). This phenomenon may be ascribed to the twisted intra molecular charge-transfer reactions [53].

Proton donating ability of solvent molecules presumably affects the solvent dependence of $\lambda_{a,max}$. It is assumed that the shoulder is due to protonated or hydrogen-bonded compounds with solvent molecule at the pyridine nitrogen [54]. The shoulder appears clearly in the hydrogen bonding donors protic solvents ethanol and methanol which has the highest proton donating ability while in the aprotic THF and DMF with no proton donating ability, respectively, the shoulders are weak [55].

4. Conclusions

Compound 2-chloro-4-(methoxymethyl)-6-methyl-5-nitropyridine-3-carbonitrile (**2**) was synthesized by novel protocol and its structure was experimentally characterized by means of X-ray Diffraction, IR, NMR and UV–vis spectroscopic spectroscopy techniques. X-ray crystal structure analysis showed that compound **2** crystallizes with two independent molecules in the asymmetric unit, which are linked separately by two different types of intermolecular interactions. A UV–vis spectrum was recorded in protic and aprotic solvents. The absorption and the emission were sensitive towards solvent polarity. The emission spectra of compound **2** exhibit strong solvent polarity dependence. Visible emission maxima of the compound showed bathocromic and hypochromic shifts, as the solvent polarity increases which results in decreased emission intensity, and the fluorescence efficiencies are reduced. Reductions of the fluorescence efficiencies, accompanied by bathochromic shifts of the emission spectra of compound **2** was depending on the protonation of the ground state and/or the excited state.

Acknowledgements

Support for this study by the Ministry of Science and Technology of Croatia (Project Nos. 058-0582261-2253 and 119-1193079-3069) is gratefully acknowledged.

Appendix A. Supplementary material

Supplementary data associated with this article can be found, in the online version, at doi:10.1016/j.molstruc.2010.06.012.

References

[1] G. Jones, in: A.R. Katritzky, C.W. Rees, E.F.V. Scriven (Eds.), Comprehensive Heterocyclic Chemistry II, vol. 5, Pergamon, Oxford, 1996.
[2] X.D. Yang, Y.Y. Yu, Struct. Chem. 19 (2008) 693.
[3] C. Ögretir, N.F. Tay, Í.Í. Öztűrk, J. Mol. Graph. Model. 26 (2007) 740.
[4] R.N. Castle, S.D. Phillips, in: A.R. Katritzky, C.W. Rees (Eds.), Comprehensive Heterocyclic Chemistry, vol. 3, Pergamon, Oxford, 1984.
[5] J.D. Figueroa-Villar, C.L. Carneiro, E.R. Cruz, Heterocycles 34 (1992) 891.
[6] P.S. Dragovich, T.J. Prins, R. Zhou, E.L. Brown, F.C. Maldonado, S.A. Fuhrman, L.S. Zalman, T. Tuntland, C.A. Lee, A.K. Patick, D.A. Matthews, T.F. Hendrickson, M.B. Kosa, B. Liu, M.R. Batugo, J.-P.R. Gleeson, S.K. Sakata, L. Chen, M.C. Guzman, J.W. Meador, R.A. Ferre, S.T. Worland, J. Med. Chem. 45 (2002) 1607.
[7] M.A.A. Bakar, N.D. Hassan, Z. Abdullah, A. Idris, Z. Aiyub, Malay. J. Anal. Sci. 12 (2008) 561.
[8] M.T. Cocco, C. Congiu, V. Onnis, Eur. J. Med. Chem. 35 (2000) 545.
[9] G.G. Danagulyan, L.G. Saakyan, G.A. Panosyan, Chem. Heterocycl. Compd. 37 (2001) 323.
[10] F. Blanco, D.H. O'Donovan, I. Alkorta, J. Elguero, Struct. Chem. 19 (2008) 339.
[11] E.A. Kaigorodova, V.K. Vasilin, E.A. Sidorova, V.E. Zavodnik, G.D. Krapivin, Chem. Heterocycl. Compd. 40 (2004) 1442.
[12] M.M. Krayushkin, I.P. Sedishev, V.N. Yarovenko, I.V. Zavarzin, S.K. Kotovskaya, D.N. Kozhevnikov, V.N. Charushin, Russ. J. Org. Chem. 44 (2008) 407.
[13] K.C. Majumdar, S. Mondal, Tetrahedron 65 (2009) 9604.
[14] R.K. Flamm, C. Vojtko, D.T. Chu, Q. Li, J. Beyer, D. Hensey, N. Ramer, J.J. Clement, S.K. Tanaka, Antimicrob. Agents Chemother. 39 (1995) 964.
[15] S. Nanjunda Swamy, B.G. Sarala, B.S. Priya, S.L. Gaonkar, J. Shashidhara Prasad, K.S. Rangappa, Bioorg. Med. Chem. Lett. 16 (2006) 999.
[16] Q. Li, D.T.W. Chu, A. Claiborne, C.S. Cooper, C.M. Lee, K. Raye, K.B. Berst, P. Donner, W. Wang, L. Hasvold, A. Fung, Z. Ma, M. Tufano, R. Flamm, L.L. Shen, J. Baranowski, A. Nilius, J. Alder, J. Meulbroek, K. Marsh, D. Crowell, Y. Hui, L. Seif, L.M. Melcher, R. Henry, S. Spanton, R. Faghih, L.L. Klein, S.K. Tanaka, J.J. Plattner, J. Med. Chem. 39 (1996) 3070.
[17] L.L. Klein, D.A. DeGoey, S.A. Thomas, C.M. Yeung, C.L. Leone, D.J. Grampovnik, D.T. Chu, P.A. Lartey, Bioorg. Med. Chem. Lett. 7 (1997) 1167.
[18] (a) W.J. Coates, Eur. Patent 351058, 1997.;
(b) W.J. Coates, Chem. Abstr. 113 (1990) 40711.
[19] (a) P. Raddatz, R. Bergmann, Ger. Patent 360731, 1988.;
(b) P. Raddatz, R. Bergmann, Chem. Abstr. 109 (1988) 54786.
[20] T.B. O'Dell, L.R. Wilson, M.D. Napoli, H.D. White, J.H. Mirsky, J. Pharmacol. Exp. Ther. 128 (1960) 65.
[21] S.A.S. Ghozlan, A.Z.A. Hassanien, Tetrahedron 58 (2002) 9423.
[22] J.A. Joule, K. Mills, Heterocyclic Chemistry, Chapman & Hall, London, 1995.
[23] H.J. Roth, A. Kleemann, Pharmaceutical Chemistry, Drug Synthesis, vol. 1, Prentice Hall Europe, London, 1988.
[24] G.D. Henry, Tetrahedron 60 (2004) 6043.
[25] N. Agarwal, P. Srivastava, S.K. Raghuwanshi, D.N. Upadhyay, S. Sinha, P.K. Shukla, V.J. Ram, Bioorg. Med. Chem. 10 (2002) 869.
[26] M.Y. Yakovlev, A.V. Kadushkin, N.P. Solov'eva, O.S. Anisimova, V.G. Granik, Tetrahedron 54 (1998) 5775.
[27] M. Jukić, M. Cetina, G. Pavlović, V. Rapić, Struct. Chem. 10 (1999) 85.
[28] M. Jukić, A. Hergold-Brundić, M. Cetina, A. Nagl, J. Vorkapić-Furač, Struct. Chem. 14 (2003) 597.
[29] M. Jukić, M. Cetina, J. Vorkapić–Furač, A. Golobić, A. Nagl, Acta Crystallogr. C59 (2003) 357.
[30] M. Cetina, M. Tranfić, I. Sviben, M. Jukić, J. Mol. Struct. 969 (2010) 25.
[31] Oxford Diffraction, Xcalibur CCD System. *CrysAlis CCD* and *CrysAlis RED*. Oxford Diffraction Ltd., Abingdon, England.
[32] G.M. Sheldrick, Acta Crystallogr. A 64 (2008) 112.
[33] A.L. Spek, J. Appl. Crystallogr. 36 (2003) 7.
[34] M. Nasr, J.C. Drach, S.H. Smith, C. Shipman, J.H. Burckhalter, J. Med. Chem. 31 (1988) 1347.

[35] H. Ban, M. Muraoka, N. Ohashi, Tetrahedron Lett. 44 (2003) 6021.
[36] T.N. Glasnov, W. Stadlbauer, C.O. Kappe, J. Org. Chem. 70 (2005) 3864.
[37] E.S. Krichevsky, L.M. Alekseeva, V.G. Granik, Chem. Heterocycl. Compd. 39 (2003) 328.
[38] S.A. Harris, K. Folkers, J. Am. Chem. Soc. 61 (1939) 1245.
[39] A.V. Guttsait, S.V. Belyakov, A.F. Mishnev, Y.Y. Bleidelis, E.Y. Gudrinietse, Khim. Geterotsikl. Soedin. (1987) 1233.
[40] M.M. Jotani, U.H. Patel, H.C. Shah, Sci. X-ray Struct. Anal. Online 22 (2006) x145.
[41] M. Bukowska-Strzyzewska, J. Skoweranda, W. Strzyzewski, R. Skowronski, J. Crystallogr. Spectrosc. Res. 21 (1991) 495.
[42] M.A. Yurovskaya, O.D. Mit'kin, V.N. Nesterov, Khim. Geterotsikl. Soedin. (1996) 680.
[43] L.-Y. Hu, H.J. Lei, D. Du, T.R. Johnson, V. Fedij, C. Kostlan, W.S. Yue, M. Lovdahl, J.J. Li, M. Carroll, D. Dettling, J. Asbill, C. Fan, K. Wade, D. Pocalyko, K. Lapham, R. Yalamanchili, B. Samas, D. Vrieze, S. Ciotti, T. Krieger-Burke, D. Sliskovic, H. Welgus, Bioorg. Med. Chem. Lett. 17 (2007) 5693.
[44] J. Bernstein, R.E. Davis, L. Shimoni, N.-L. Chang, Angew. Chem. Int. Ed. 34 (1995) 1555.
[45] I. Alkorta, S. Maluendes, J. Phys. Chem. 99 (1995) 6457.
[46] T. Steiner, Crystallogr. Rev. 9 (2003) 177.
[47] C.A. Hunter, J.K.M. Sanders, J. Am. Chem. Soc. 112 (1990) 5525.
[48] J. Hanuza, M. Mączka, A. Waśkowska, W. Oganowski, H. Ban-Oganowska, B. Lutz, J.H. van der Maas, Vib. Spectrosc. 14 (1997) 49.
[49] J. Hanuza, M. Mączka, A. Waśkowska, W. Oganowski, H. Ban-Oganowska, E.T.G. Lutz, J.H. van der Maas, J. Mol. Struct. 450 (1998) 201.
[50] G.G. Guilbault, Practical Fluorescence, Marcel Dekker, New York, 1990.
[51] P.S. Kalsi, Spectroscopy of Organic Compounds, New Age International Publishers, New Delhi, 2004.
[52] T. Basché, W.E. Moerner, M. Orrit, U.P. Wild, Single-molecule Optical Detection, Imaging and Spectroscopy, VCH, Weinheim, 1997.
[53] L.D.S. Yadav, Organic Spectroscopy, Kluwer Academic Publishers, Dordrecht, 2005.
[54] C. Reichardt, Solvents and Solvent Effects in Organic Chemistry, Wiley-VCH, Weinheim, 2003.
[55] D.Ž. Mijin, G.S. Uščumlić, N.U. Perišić-Janjić, N.V. Valentić, Chem. Phys. Lett. 418 (2006) 223.